



CHORUS

This is the accepted manuscript made available via CHORUS. The article has been published as:

Chain Conformation in Polymer Nanocomposites with Uniformly Dispersed Nanoparticles

M. K. Crawford, R. J. Smalley, G. Cohen, B. Hogan, B. Wood, S. K. Kumar, Y. B. Melnichenko, L. He, W. Guise, and B. Hammouda

Phys. Rev. Lett. **110**, 196001 — Published 6 May 2013

DOI: [10.1103/PhysRevLett.110.196001](https://doi.org/10.1103/PhysRevLett.110.196001)

Chain Conformation in Polymer Nanocomposites with Uniformly Dispersed Nanoparticles

M.K. Crawford,¹ R.J. Smalley,¹ G. Cohen,¹ B. Hogan,¹ B. Wood,¹ S.K. Kumar,² Y.B. Melnichenko,³ L. He,³ W. Guise,^{1,4} and B. Hammouda⁵

¹DuPont Central Research and Development Department, E400/5424,
Wilmington, DE 19880-0400

²Department of Chemical Engineering, Columbia University, New York, N.Y 10027

³Biology and Soft Matter Division, Oak Ridge National Laboratory,
Oak Ridge, TN 37831-6393

⁴Advanced Photon Source, Argonne National Laboratory,
9700 S. Cass Ave, Lemont, IL 60439

⁵NIST Center for Neutron Research, Gaithersburg, MD 20879-8562

Abstract

The effect of nanoparticles (NP) on chain dimensions in polymer melts has been the source of considerable theoretical and experimental controversy. We exploit our ability to ensure a spatially uniform dispersion of 13 nm silica NPs miscible in polystyrene melts, together with neutron scattering, x-ray scattering and transmission electron microscopy (TEM), to show that there is no measurable change in the polymer size in miscible mixtures, regardless of the relative sizes of the chains and the nanoparticles, and for NP loadings as high as 32.7 volume %. Our results provide a firm basis from which to understand the properties of polymer nanocomposites.

PACS 83.85.Hf, 83.80.Tc, 82.35.Np

Polymer nanocomposites (PNC), formed by adding nanoparticles (NPs) to polymers, can have crucially improved physical properties relative to the pure polymer [1]. We focus here on a fundamental question – Do chain sizes change on adding NPs to a polymer and what controls this behavior? For very small NPs, the PNCs should be analogous to concentrated polymer solutions, where theories and experiments agree that polymer chains can expand, collapse, or be unaffected, depending upon the NP-solvent interaction and polymer concentration [2, 3]. For PNCs, however, theories qualitatively disagree on the role of NPs on chain size [4-13], even in the athermal limit.

On the experimental side, there are multiple examples where neutron scattering has been used to characterize the polymer radius of gyration, R_g , in PNC: (i) 13 nm silica NPs did not change the R_g of polystyrene (PS, both $R_g < R_p$ and $R_g > R_p$) for NP loadings as high as 27 volume %, but transmission electron microscopy (TEM) images showed poor NP dispersion [14, 15]. (ii) Similar 13 nm NPs in polyethylenepropylene did not change R_g when $R_g < R_p$, but a 12% *contraction* occurred when $R_g > R_p$ at 50 volume % NP loading [16]. No TEM data were presented. Two studies using smaller NPs found significant chain expansions, perhaps signaling a cross-over to solvent-like behavior: (iii) A study [17] of PS chains with soft cross-linked PS NPs ($R_p \approx 2$ to 4 nm) found PNC miscibility and chain expansion by as much as 20% when $R_g \geq R_p$ at 10 volume % NP loading. The chains and NP were immiscible for $R_g < R_p$. (iv) Soft polysilicate NPs with radius $R_p = 1$ nm were found to expand polydimethylsiloxane chains by as much as 60% for NP loadings of 40 volume % when $R_g > R_p$ [18]. However, the quality of the NP spatial dispersions was not reported. Thus, the experimental results suggest no swelling for 13 nm diameter NPs, independent of the ratio of polymer R_g to NP size, but good miscibility was not achieved; NP-polymer miscibility and significant swelling for 4-8 nm diameter NPs when $R_g \geq R_p$; and dramatic swelling of long chains in the presence of very small 2 nm diameter NPs when $R_g > R_p$. Importantly, it is implied that NP miscibility

and polymer chain swelling are directly related, and the controlling parameter is the ratio R_g/R_p [17, 19].

This Letter remedies the major deficiency of the earlier studies for hard NPs by only dealing with PNCs with well-dispersed 13 nm diameter silica NPs, as shown by ultrathin section TEM images. We then combine small angle x-ray (SAXS) and neutron (SANS) scattering to definitively demonstrate that, for $R_p < R_g$, NPs have no measurable effect on polymer conformation, independent of polymer molecular weight and NP concentration. We do not examine cases with $R_g \leq R_p$ because, in agreement with a prior study [17], we find that these PNCs phase separate.

Table 1 lists the characteristics of the polymers used in our study. The reported diameter of 13 nm for the silica NPs (supplied by Nissan Chemical) is in good agreement with our dilute solution SAXS results (not shown), which also yield a silica NP polydispersity of 0.31. Separate solutions of PS and silica NPs in N,N-dimethylformamide (DMF), a theta to good solvent for PS [20, 21], were mixed. Silica NPs are charged in DMF [21, 22], and so charge stabilization may help in attaining good dispersion [23], although arguments showing it is not very important for 30 nm diameter (and smaller) NPs have been given [21]. A unique feature of our work is that the silica surfaces are treated with trimethoxyphenylsilane; thus the surface hydroxyls are replaced with phenylsilane groups. The resulting silane surface coating density, determined by thermogravimetric analysis (TGA), was $4.5 \times 10^{-4} \text{ g/m}^2$ (2.9 silanes/nm²). These phenyl-containing end-groups are more compatible with non-polar PS, and are probably crucial to the excellent NP dispersions achieved (Figure 1). Here, we also note that PS chains do not adsorb on bare silica in DMF [24]. SANS data for the silica NPs in mixtures of deuterated and hydrogenated isopropyl alcohol did not show the core-shell scattering that was found in [16] with different surface functional groups. This is probably due to the very thin silane surface layers on our NPs.

By using various mixtures of deuterated and hydrogenated isopropyl alcohol (contrast variation) we determined the neutron scattering length density (SLD) of the functionalized silica NPs to be $3.0 \times 10^{-6} \text{ \AA}^{-2}$. The same NPs without the silane surface treatment had a measured SLD of $3.47 \times 10^{-6} \text{ \AA}^{-2}$, consistent with fully dense silica (2.2 g/cm^3). The polymer matrices [68 volume % h-PS/32 volume % d-PS (SLD = $3.1 \times 10^{-6} \text{ cm}^{-2}$)] were approximately contrast matched to the NPs. The polymer/silica solutions were cast as $\sim 300 \text{ \mu m}$ thick films on a glass plate heated to $100\text{-}120 \text{ }^\circ\text{C}$ to ensure rapid solvent evaporation. The films were then annealed for approximately 16 hours at $140 \text{ }^\circ\text{C}$ in vacuum to remove residual solvent [25]. Several films were then stacked and hot pressed together to yield the final $\sim 1 \text{ mm}$ thick SANS samples. When the polymer $R_g > R_p$, uniform dispersions were obtained, while the dispersions showed clear evidence for fluid-fluid phase separation when $R_g \leq R_p$ (Fig. 1e) [21, 26]. We do not have an explanation for why the low molecular weight mixtures phase separate and the high molecular weight mixtures do not. Theory suggests similar equilibrium phase behavior for both [26], so the difference may be due to slower phase separation kinetics at higher polymer molecular weights in the rapidly evaporating solvent [23]. However, we do not consider the phase-separated samples further. Several of the hot pressed samples exhibited small anisotropy in their 2-D SANS patterns, but only at low q . SANS data were collected on beamline NG-7 at the NIST Center for Neutron Research and on beamlines CG-2 and CG-3 at the High Flux Isotope Reactor at Oak Ridge National Laboratory for $q (= 4\pi\sin\theta/\lambda)$ values from 0.001 \AA^{-1} to 0.5 \AA^{-1} . SAXS data were collected over $q = 0.002 \text{ \AA}^{-1}$ to 0.5 \AA^{-1} on an insertion device beamline located at the DND-CAT sector of the Advanced Photon Source at Argonne National Laboratory.

Figure 2 shows SANS and SAXS data for PNCs of 200 kDa PS with different NP loadings (Table I). The SANS data have been normalized by the volume fraction of

polymer to collapse them onto a “universal” $I(q) \sim q^{-2}$ dependence expected at intermediate q for Gaussian chains described by the Debye form factor. This shows that the contrast matching of the silica NPs and the polymer matrix reveals primarily single chain scattering. This point is more clearly shown by comparing the SAXS data with the SANS data (Fig. 2). The scattering contrast for SAXS is due to the difference in electron density between the polymer matrix and the silica, and thus the intensity is proportional to the product of the form and structure factors for the silica nanoparticles only. Fig. 2b shows that the SAXS intensities at high q scale as q^{-4} (Porod scattering) due to well defined NP/polymer interfaces. At low q the SAXS intensity *decreases* with increasing NP loading, as expected for a hard sphere structure factor.

In contrast, the low q SANS intensity *increases* with NP loading. This is unexpected since the NPs have been contrast matched to the polymer. A NP contribution to the scattering would be present, however, if the contrast match was not perfect, if the scattering length density of the silica nanoparticles was not homogenous [16], or if different NPs had slightly different SLD due to particle-to-particle variations. A small mismatch of the SLD would be less apparent at high q , where the NP scattering is rapidly decreasing as $I(q) \sim q^{-4}$, as seen for the SAXS data (Fig. 2). If the NP are indeed contrast matched, then the trend that the SANS intensity increases with silica concentration at low q likely originates from changes of the polymer structure factor, similar to predictions based upon the PRISM theory [27]. The increase of the SANS intensity at low q might then suggest that the system is close to phase separation driven by the NP-polymer interactions. The phase separation observed for the low molecular weight polymers would then be a manifestation of this tendency. (It should be noted that the molecular weights of the polymers we have studied are too low to lead to phase separation due to isotopic substitution [28]). Further work is needed to understand this phenomenon in detail, but its presence even in the better dispersions invalidates the use

of a simple Guinier analysis of the SANS data to extract values for polymer R_g . Instead, as in several previous studies [14, 16], we use the intermediate q SANS data to evaluate the role of silica NPs on R_g .

Figure 3 (inset) shows Kratky plots [$q^2 I(q)$ vs q] of the SANS data for one set of PNCs with different concentrations of silica NP. The raw intensity data were first divided by the volume fraction of polymer, and then the incoherent scattering subtracted. Because of this procedure, the incoherent contribution was found to be similar across samples, as expected. The Kratky plots show plateaus at intermediate q , clearly demonstrating that the polymer chains always remain Gaussian. In addition, since the Kratky plateaus are independent of silica concentration, it then follows that the values of chain statistical segment length (proportional to the inverse of the square-root of the plateau) and the R_g are also constant. This is our primary result (Fig. 3). Figure 3 also shows that these results are reproducible on two different SANS instruments at Oak Ridge National Laboratory.

We now attempt to reconcile our results with the widely varying literature trends discussed in the Introduction. We first note that all the data on hard NPs of diameter ~ 13 nm [14-16], appear to be internally consistent and show either no, or at most small, changes in polymer size on the addition of NPs up to 50 volume %. However, these previous studies utilized samples that either had poor or uncharacterized states of filler dispersion. Our study goes beyond these earlier measurements by using well dispersed hard NPs, as demonstrated by TEM and SAXS, providing convincing evidence that *in this size range* $1.2 < R_g/R_p < 4.1$ (Table 1) *there are no changes in chain dimensions*. For smaller R_g/R_p the NPs are not miscible with the polymer, in agreement with [17, 19]. In reference [17] chain expansion was found for samples whose R_g/R_p ratios varied between 1.6 and 5.7, and in reference [18] expansion was found for R_g/R_p values between 3 and 10. The significant chain swelling observed in [17-19] for 2 to 8 nm NPs,

word_XW1E7gZ4qvv53RCwMMQ9.doc

and the absence of chain swelling for 13 nm NPs in PNC with similar R_g/R_p ratios, shows that the value of this ratio alone does not control chain swelling. Thus we must conclude that polymer R_g is not the relevant length scale below which NPs swell polymer chains. Whether the swelling induced by very small NPs signals a crossover to solvent-like behavior remains an open question.

A portion of this research at Oak Ridge National Laboratory's High Flux Isotope Reactor was sponsored by the Scientific User Facilities Division, Office of Basic Energy Sciences, U. S. Department of Energy. Use of the Advanced Photon Source, an Office of Science User Facility operated for the U.S. Department of Energy (DOE) Office of Science by Argonne National Laboratory, was supported by the U.S. DOE under Contract No. DE-AC02-06CH11357. SK thanks the National Science Foundation (DMR-1006514) for partial support of this research. We acknowledge the support of the National Institute of Standards and Technology, U.S. Department of Commerce, in providing the neutron research facilities used in this work. This work utilized facilities supported in part by the National Science Foundation under Agreement No. DMR-0944772. The identification of commercial products does not imply endorsement by the National Institute of Standards and Technology nor does it imply that these are the best for the purpose.

References

1. J. Jancar et al., *Polymer* **51**, 3321 (2010)
2. J. des Cloizeaux and G. Jannink, "Polymers in Solution: Their Modeling and Structure", Oxford University Press, New York (2010).
3. P.G. de Gennes, "Scaling Concepts in Polymer Physics", Cornell University Press, Ithaca (1979)
4. G. Allegra, G. Raos, and M. Vacatello, *Prog. Polym. Sci.* **33**, 683 (2008) and references therein.
5. Q.W. Yuan, A. Kloczkowski, J.E. Mark and M.A. Sharaf, *J. Poly. Sci.:Part B: Polymer Physics* **34**, 1647 (1996)
6. A.L. Frischknecht, E.S. McGarrity, and M.E. Mackay, *J. Chem. Phys.* **132**, 204901 (2010)
7. M.A. Sharaf and J.E. Mark, *Polymer* **45**, 3943 (2004)
8. M. Vacatello, *Macromolecules* **35**, 8191 (2002)
9. Y. Termonia, *Polymer* **50**, 1062 (2009)
10. G.G. Voyiatzis, E. Voyiatzis, and D.N. Theodorou, *Europ. Poly. J.* **47**, 699 (2011)
11. A. Ghanbari et al., *Macromolecules* **45**, 572 (2012)
12. D. Wu, K. Hui, and D. Chandler, *J. Chem. Phys.* **96**, 835 (1991)
13. R.P. Sear, *Phys. Rev. E* **66**, 051401 (2002)
14. S. Sen et al., *Phys. Rev. Lett.* **98**, 128302 (2007)
15. N. Jouault et al., *Macromolecules* **43**, 9881 (2010)
16. K. Nusser et al., *Macromolecules* **43**, 9837 (2010)
17. A. Tuteja et al., *Phys. Rev. Lett.* **100**, 077801 (2008)
18. A.I. Nakatani et al., *Polymer* **42**, 3713 (2001)
19. M.E. Mackay, A. Tuteja, P.M. Duxbury, C.J. Hawker, B. Van Horn, Z. Guan, G. Chen, and R.S. Krishnan, *Science* **311**, 1740 (2006)

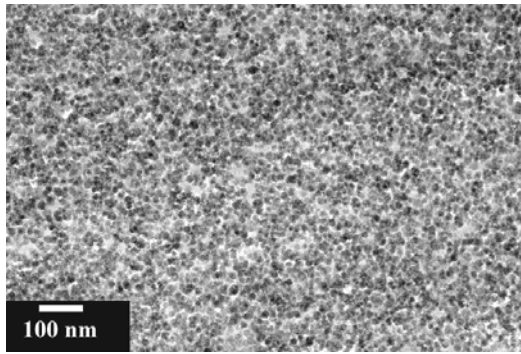
word_XW1E7gZ4qvv53RCwMMQ9.doc

20. B.A. Wolf and M.M. Willms, *Makromol. Chem.* **179**, 2265 (1978)
21. J. Zhou, J.S. van Duijneveldt, and B. Vincent, *Langmuir* **26**, 9397 (2010)
22. J. Gapinski et al., *J. Chem. Phys.* **130**, 084503 (2009); J. Gapinski, A. Patkowski, and G. Negele, *J. Chem. Phys.* **132**, 054510 (2010)
23. J.S. Meth et al, *Macromolecules* **44**, 8301 (2011)
24. T. Cosgrove, *J. Chem. Soc. Faraday Trans.* **86**, 1323 (1990)
25. A. Bansal et al., *J. Polym. Sci. : Part B : Polym. Phys.* **44**, 2944 (2006)
26. H.N.W. Lekkerkerker and R. Tuinier, "Colloids and the Depletion Interaction", Springer, New York (2011)
27. J.B. Hooper and K.S. Schweizer, *Macromolecules* **40**, 6998 (2007)
28. F.S. Bates and G.D. Wignall, *Macromolecules* **19**, 932 (1986)

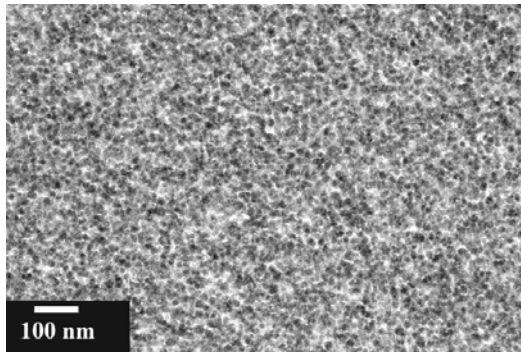
Table 1. Polymers and polymer nanocomposite compositions used in this study. The values for the polymer molecular weights and polydispersities were supplied by the manufacturers (Polymer Source and Varian). The R_g values for the hydrogenated and deuterated polymers were determined by fits of the random phase approximation expression [3] for the q dependent neutron scattering intensity (structure factor) to the SANS data for unfilled isotopic blends.

| Molecular Weight (kDa) | | Polydispersity (M_w/M_n) | | R_g (nm), unfilled | | R_g/R_p | | Silica volume fractions | Average Surface-to-Surface Interparticle Spacing (nm) |
|------------------------|-------|------------------------------|------|----------------------|------|-----------|------|-------------------------|---|
| h-PS | d-PS | h-PS | d-PS | h-PS | d-PS | h-PS | d-PS | | |
| 49.9 | 47.4 | 1.03 | 1.02 | 5.49 | 5.24 | 0.84 | 0.81 | 0 | --- |
| | | | | | | | | 0.1 | 11 |
| | | | | | | | | 0.2 | 6.1 |
| | | | | | | | | 0.3 | 3.6 |
| 96.6 | 96.4 | 1.02 | 1.02 | 7.44 | 7.42 | 1.14 | 1.14 | 0 | --- |
| | | | | | | | | 0.1 | 11 |
| | | | | | | | | 0.2 | 6.1 |
| | | | | | | | | 0.3 | 3.6 |
| 194.1 | 231 | 1.03 | 1.03 | 13.1 | 12.2 | 1.95 | 2.11 | 0 | --- |
| | | | | | | | | 0.078 | 13 |
| | | | | | | | | 0.087 | 12 |
| | | | | | | | | 0.212 | 6 |
| 493.3 | 479.8 | 1.03 | 1.09 | 20.9 | 19.3 | 3.23 | 3.03 | 0 | --- |
| | | | | | | | | 0.078 | 13 |
| | | | | | | | | 0.212 | 6 |
| | | | | | | | | 0.327 | 3 |
| 637 | 690 | 1.05 | 1.05 | 24.3 | 23.9 | 3.69 | 3.68 | 0 | --- |
| | | | | | | | | 0.221 | 6 |
| | | | | | | | | 0.327 | 3 |
| 764.5 | 690 | 1.04 | 1.05 | 25.5 | 22.9 | 4.11 | 3.68 | 0 | --- |
| | | | | | | | | 0.078 | 13 |

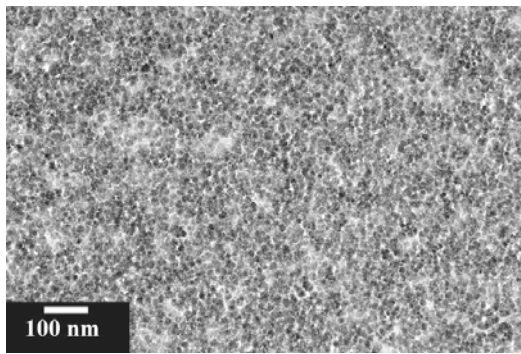
a)



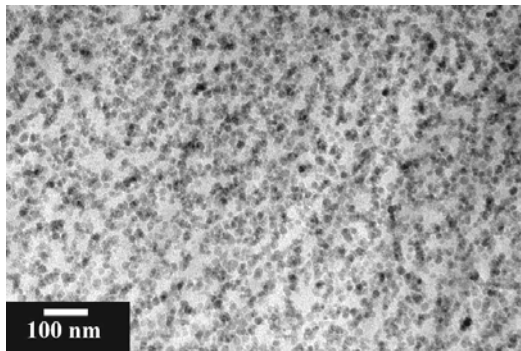
b)



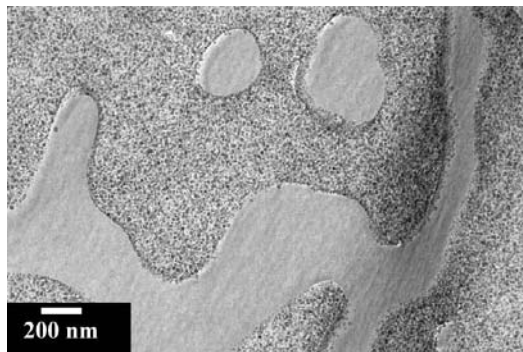
c)



d)



e)



f)

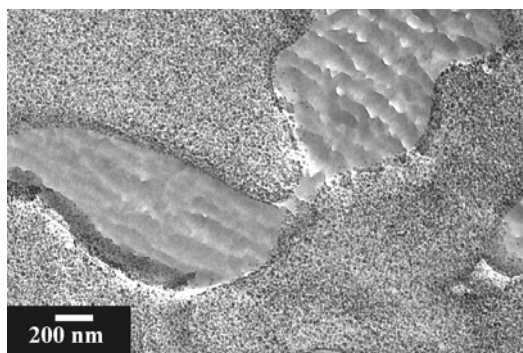


Figure 1. TEM images of nanocomposites composed of a) 32.7 volume % silica NP in 194 kDa h-PS/231 kDa d-PS; b) 32.7 volume % silica NP in 493 kDa h-PS/480 kDa d-PS; c) 32.7 volume % silica in 637 kDa h-PS/690 kDa d-PS; d) 8.7 volume % silica in 194 kDa h-PS/231 kDa d-PS; e) 13 volume % 13 nm silica NP in 97 kDa h-PS; f) 13 volume % 13 nm silica NP in 49 kDa h-PS. In images e and f there are regions of polystyrene without NP which show clear evidence of compression ridges, ruling out the interpretation that they are due to air bubbles. Although the PNCs imaged in e and f were composed of pure h-PS plus silica NP, similar phase behavior was observed in isotopic mixtures with the polymer molecular weights given in Table 1.

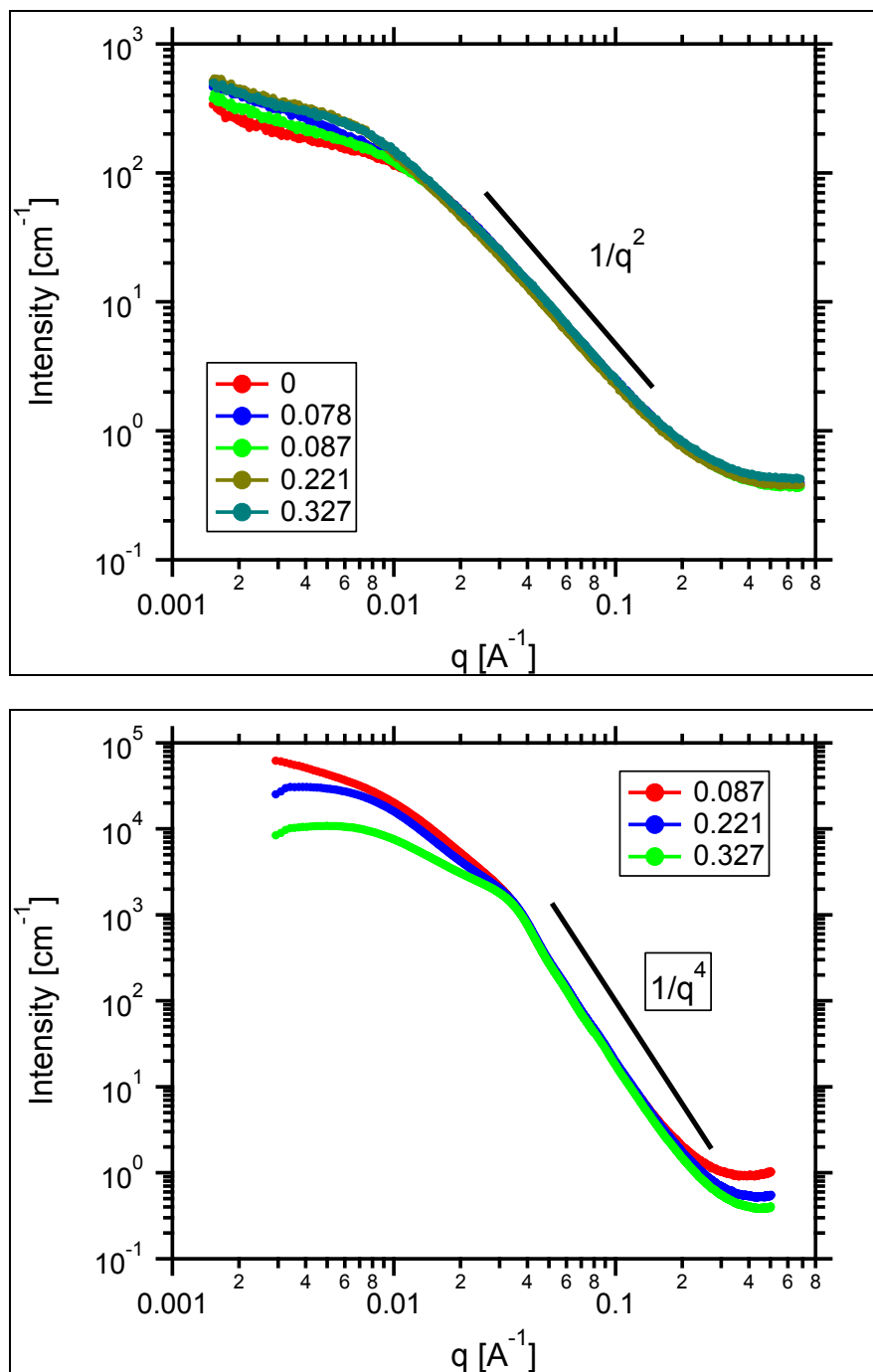


Figure 2. Log-log plots of SANS (top) and SAXS (bottom) data for a series of polymer nanocomposites composed of 0.68 volume fraction 194 kDa h-PS and 0.32 volume fraction 231 kDa d-PS with the volume fractions of silica nanoparticles shown in the legends. The SANS data are normalized by the volume fraction of polymer in each sample, whereas the SAXS data have been normalized by the volume fraction of silica in each sample.

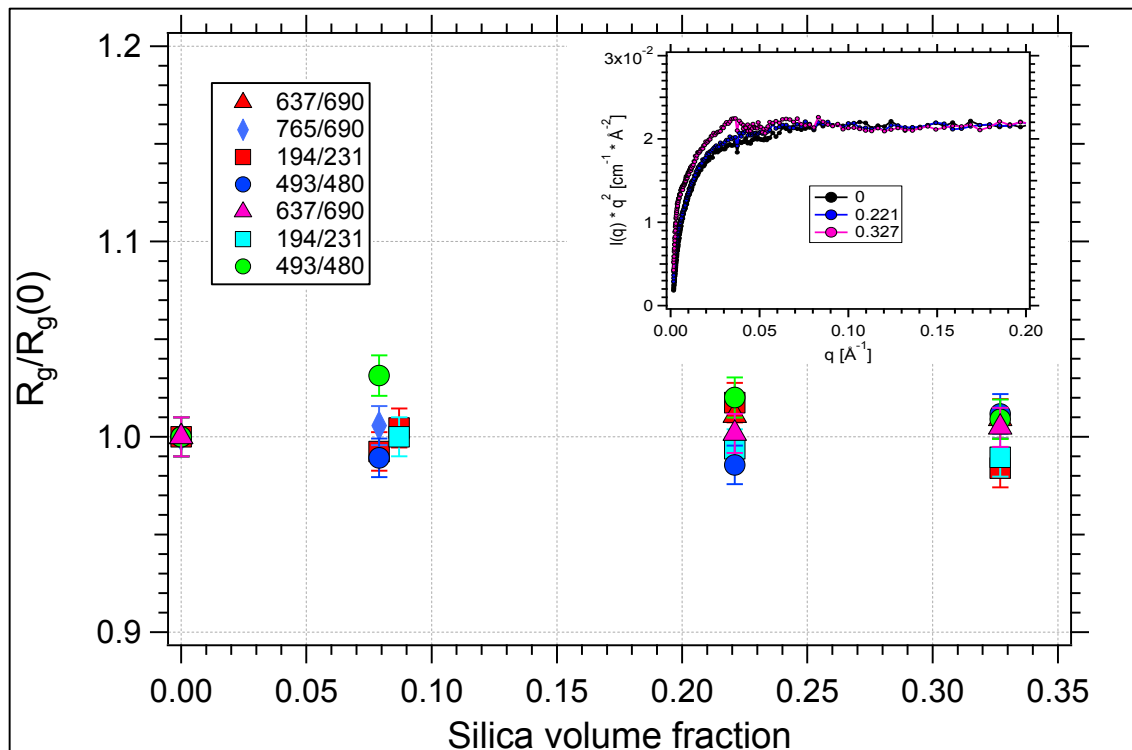


Figure 3. Variation of polymer R_g with silica volume fraction for 0.68 volume fraction h-PS/0.32 volume fraction d-PS blends with different polymer molecular weights shown in the legend. The R_g values for the nanocomposites have been normalized by the R_g values for the unfilled polymers. The statistical error bars represent one standard deviation in the determinations of the values of the Kratky plateaus for the individual data sets. Data for samples that were characterized twice on different SANS instruments are shown with identical symbols of different color, and their comparison suggests that the measurement accuracy is approximately $\pm 5\%$.

(inset) Kratky plots for 13 nm silica NP contrast matched with 637 kDa h-PS/690 kDa d-PS. The silica volume fractions are listed in the legends. The data are normalized by the volume fraction of polymer in each sample, and the incoherent background was subtracted from each data set.